

## Rationalization of the $\pi$ – $\sigma$ (Anti)aromaticity in All Metal Molecular Clusters

Ayan Datta and Swapan K. Pati\*

*Theoretical Sciences Unit and Chemistry and Physics of Materials Unit, Jawaharlal Nehru Center for Advanced Scientific Research, Jakkur P. O, Bangalore-560064, India*

Received May 20, 2005

**Abstract:** A  $\sigma$ – $\pi$  separation analysis of the energies in  $\text{Al}_4\text{Li}_4$  reveals that the system is more  $\pi$ -antiaromatic than the  $\sigma$ -aromaticity in it. This is true also for  $\text{C}_4\text{H}_4$  and  $\text{Ga}_4\text{Li}_4$ . Unlike  $\text{C}_4\text{H}_4$  that has a very large component of  $\pi$ -antiaromaticity, for these all-metal clusters, these energy scales are comparable though  $\pi$ -antiaromaticity is the major driving force for the distortion of the molecules from the square ( $\sigma$ -aromatic) structure to the rectangular ( $\pi$ -antiaromatic) architecture. For the dianion  $\text{Al}_4\text{Li}_4^{2-}$ , the  $\sigma$ -equalization prevails over the  $\pi$ -distortion in  $\text{Al}_4\text{Li}_4$ , and for the dication  $\text{Al}_4\text{Li}_4^{2+}$ ,  $\pi$ -equalization is the driving force for the square symmetric structure.

The past decade has witnessed rapid progress in the new chemistry of small metal clusters of Al, Si, and Ga facilitated by computational strategy, synthesis, and characterization.<sup>1–3</sup> These metal clusters have a close resemblance with the cyclic organic  $\pi$ -conjugated molecules in structure as well as properties.  $\text{Al}_4\text{Li}_4$  and their anions,  $\text{Al}_4\text{Li}_3^-$  or  $\text{Al}_4^{4-}$ , follow the properties of cyclobutadiene ( $\text{C}_4\text{H}_4$ ).<sup>4</sup> They also undergo interaction with transition metals such as Fe and Ni to form complexes of the type  $(\text{Al}_4\text{Li}_4)\text{-Fe}(\text{CO})_3$  and sandwich complexes of the type  $(\text{Al}_4\text{Li}_4)_2\text{Ni}$  thereby resembling  $\text{C}_4\text{H}_4$  in its role as a ligand.<sup>5</sup>  $\text{Al}_4^{4-}$  also satisfies the simple Hückel criteria for antiaromaticity as it possesses  $4\pi$  electrons in its frontier  $\pi$ -orbitals. Despite the similarities between these all-metal systems and their organic counterpart ( $\text{C}_4\text{H}_4$ ), serious doubts have recently been raised whether these systems are aromatic or antiaromatic, based on the  $\pi$ -electron scheme alone.<sup>6,7</sup> The  $\sigma$ -backbone appears to be quite important and based on a nucleus independent chemical shift (NICS), Schleyer and co-workers suggested that these clusters are net aromatic. But Boldyrev, Wang, and co-workers concluded that  $\text{Li}_3\text{Al}_4^-$  and  $\text{Li}_4\text{Al}_4$  clusters are net antiaromatic. Santos and co-workers agreed with the net antiaromaticity of these clusters on the basis of electron localization function (ELF) analysis.<sup>8</sup>

In this letter we show that the confusion associated with these clusters can be settled through a simple  $\sigma$ – $\pi$  separation analysis which provides an unambiguous answer to all such

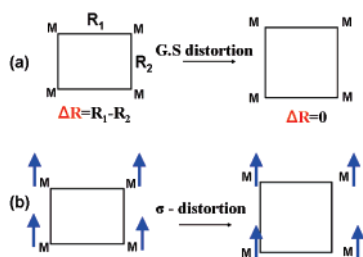
questions. The different results obtained by the previous workers arise primarily because of the indirect methods used to characterize aromaticity/antiaromaticity. We stress that the  $\sigma$ -backbone is quite an important component in the structural features of almost all molecular systems. Even in  $\text{C}_6\text{H}_6$ , it has been found that the  $\sigma$ -backbone is responsible for the symmetric  $D_{6h}$  structure and the  $\pi$ -electrons actually tend to distort the symmetric structure.<sup>9,10</sup>

We have considered a variety of molecular systems,  $\text{Al}_4\text{-Li}_4$ ,  $\text{Al}_4\text{Li}_4^{2-}$ ,  $\text{Ga}_4\text{Li}_4$ , and  $\text{Al}_4^{2-}$ , and compared with  $\text{C}_4\text{H}_4$  and similar organic analogues at each step of our  $\sigma$ – $\pi$  analysis. These systems have either  $4\pi$ ,  $6\pi$ , or  $2\pi$  electrons in their frontier orbitals and provide a diverse set for studying aromaticity or antiaromaticity. All the geometries were optimized at the B3LYP/6-311G++ (d, p) level<sup>11,12</sup> (see the Supporting Information file for structures and energies). The ground-state geometry for both  $\text{Al}_4\text{Li}_4$  and  $\text{Ga}_4\text{Li}_4$  have a planar rectangular structure for the ring with the Li ions occupying positions so as to maintain a  $C_{2h}$  architecture. The bond-length alteration (BLA) for  $\text{Al}_4\text{Li}_4$  and  $\text{Ga}_4\text{Li}_4$  are 0.12 and 0.16 Å, respectively. Note that the same for  $\text{C}_4\text{H}_4$  is 0.2 Å. The fact that the BLA for  $\text{Ga}_4\text{Li}_4$  is more than that in  $\text{Al}_4\text{Li}_4$  suggests that  $\text{Ga}_4\text{Li}_4$  is more antiaromatic than  $\text{Al}_4\text{-Li}_4$ , in analogy with  $\text{C}_4\text{H}_4$ , and a  $\sigma$ – $\pi$  separation should be ideal to quantify such a statement.

We distort the geometry optimized structures by  $\Delta R$  (where  $\Delta R$  is the difference between the long M–M and short M–M bond in the  $\text{M}_4$  ring) so that that the distortion keeps the sum of two adjacent M–M bonds constant

\* Corresponding author e-mail: pati@jncasr.ac.in.

**Scheme 1.** (a) Distortion Mode for the  $M_4$  Rings ( $M=C$ , Al, Ga) in the Ground State<sup>a</sup> and (b) Distortion in the  $\sigma$ -Electrons Involving the Distortion in a High-Spin Configuration



<sup>a</sup> Li atoms not shown for the sake of clarity.

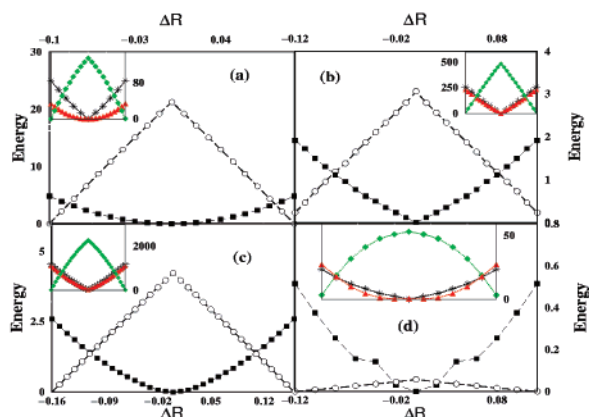


**Figure 1.** Variation of the  $\sigma$ -energy (square) and the  $\pi$ -energy (circles), both in kcal/mol as a function of the distortion axis,  $\Delta R$  for (a)  $C_4H_4$ , (b)  $Al_4Li_4$ , (c)  $Ga_4Li_4$ , and (d)  $Al_4Li_4^{2-}$  derived from  $(Al_4Li_4)Fe(CO)_3$ . The insets show  $V_{core}$  (green),  $V_{ee}$  (black), and  $V_{nn}$  (red) components in the ground-state structures. All the energies are scaled to make the most stable geometry zero in energy and positive values in the energy-axis correspond to destabilization.

[Scheme 1 (a)]. The energy associated with the distortion is partitioned into  $\sigma$  and  $\pi$  components as  $\Delta E_{\pi} = \Delta E_{GS} - \Delta E_{\sigma}$ . One of the simplest methods to get the contribution associated with a distortion only along the  $\sigma$ -backbone is to freeze the  $\pi$ -electrons with all-parallel spins. The  $\sigma$ -backbone for a  $M_4$  ring with  $4\pi$  electrons can be modeled as  $M_4^{4-}$  with a high spin configuration ( $S = 2$ ) with all the  $4\pi$  electrons being parallel [Scheme 1(b)]. Similarly, for the  $2\pi$  electron systems such as  $C_4H_4^{2+}$  and  $Al_4^{2-}$ ,  $S = 1$  corresponds to the high spin state. For the  $6\pi$   $Al_4Li_4^{2-}$  however, there are only four  $\pi$ -orbitals and thus a high spin configuration with  $S = 3$  is not feasible, rather two parallel spins with  $S = 1$  state in  $Al_4Li_4^{2-}$  corresponds to the high spin state. We thus define,  $\Delta E_{\sigma} = \Delta E_{HS}$ . Such an analysis gives a very clear picture of the nature of interactions in the system and has been extensively used in the literature for various organic molecules.<sup>13,14</sup> For the high spin systems, we perform UB3LYP calculations at the same basis set level with annihilation of the first spin-contaminant.

In Figure 1, we plot the  $\sigma$ -energy and the  $\pi$ -energy as a function of the distortion parameter,  $\Delta R$ . In the inset, the core energy,  $V_{core}$  (sum of kinetic energy and nuclear-electron (ne) interactions), electron–electron interactions ( $V_{ee}$ ), and

the nuclear–nuclear interactions ( $V_{nn}$ ) are plotted. For all the systems, we find that the  $\pi$ -electrons have a general tendency of forming a distorted structure ( $\pi$ -energy is most stable at large  $\Delta R$ ), while the  $\sigma$ -framework opposes the distortion and tends to equalize the bonds. The final structure and thus the aromatic/antiaromatic features will crucially depend on the predomination of either of the forces. In Figure 1(a), the result for the well-known  $C_4H_4$  system is shown. The instability associated with the  $\sigma$ -backbone distortion is very little (4 kcal/mol for  $\Delta R = 0.1$ ), while the stability for  $\pi$ -distortion is quite substantial (22 kcal/mol for  $\Delta R = 0.1$ ), clearly overwhelming the tendency for  $\sigma$ -backbone equalization. Thus the  $C_4H_4$  has a rectangular structure and is overall  $\pi$ -antiaromatic with a minor  $\sigma$ -aromatic component. Both  $V_{ee}$  and  $V_{nn}$  are destabilized with distortion, while the  $V_{core}$  component is stabilized. We have further analyzed that it is the  $V_{ne}$  term in the  $V_{core}$  that favors the distorted structure. This is easy to understand as the  $V_{ne}$  component is associated with the electron–lattice interactions and leads to the Jahn–Teller stabilization in the distorted structure. However components such as  $V_{ee}$  and  $V_{nn}$  stabilizes the  $\Delta R = 0$  structure associated with the delocalized  $\pi$ -electrons (for nonzero  $\Delta R$ , the electron density is localized in shorter bonds).

For the all-metal system however, the  $\sigma$ – $\pi$  separation energy plays a crucial role. For example, in  $Al_4Li_4$ , the distortion in the  $\sigma$ -framework leads to a destabilization of 2.5 kcal/mol, while the  $\pi$ -framework gains energy of 3.5 kcal/mol (Figure 1(b)). The ground-state energy is thus stabilized by the distortion along the ring. Accordingly thus the  $Al_4Li_4$  is  $\pi$ -antiaromatic though the  $\sigma$ -aromatic component is also substantial. However overall  $Al_4Li_4$  is antiaromatic as the  $\pi$ -antiaromaticity exceeds the  $\sigma$ -aromaticity by 1 kcal/mol. The energy components also follow very similar trends such as that for  $C_4H_4$  (Figure 1(b), inset). We derive a similar conclusion for the  $Ga_4Li_4$  also; the  $\pi$ -stabilization associated with the distortion is 4 kcal/mol, while  $\sigma$ -destabilization is 2.5 kcal/mol (seen in Figure 1(c)). The distorted  $\pi$ -antiaromatic structure is thus stabilized by an amount of 1.5 kcal/mol, 0.5 kcal/mol more than that for  $Al_4Li_4$ . Thus the  $\pi$ -antiaromaticity follows the order  $C_4H_4 > Ga_4Li_4 > Al_4Li_4$ .

The fact that this simple  $\sigma$ – $\pi$  separation gives a very clear picture for the nature of aromaticity/antiaromaticity is evident from Figure 1(d). We retrieve the structure of the  $Al_4Li_4$  unit from the organometallic complex  $(Al_4Li_4)Fe(CO)_3$  and consider the  $Al_4Li_4$  dianion system. The interaction of the  $Fe(CO)_3$  unit with the  $Al_4Li_4$  converts it into a  $6\pi$  aromatic system with small BLA. In Figure 1(d) we distort this dianion of  $Al_4Li_4$  and perform a similar analysis. Contrary to the previous cases, in  $Al_4Li_4^{2-}$ , the stabilization associated with the equalization of the  $\sigma$ -backbone overwhelms the instability due to  $\pi$ -electron localization by 0.5 kcal/mol and forces the system to be aromatic. This is of course true for  $C_6H_6$  where  $\sigma$ -delocalization exceeds the  $\pi$ -localization by 6 kcal/mol.<sup>15,16</sup> In Figure 2 (a), the energy profile is plotted for  $C_4H_4^{2+}$  which shows an overwhelming  $\pi$ -delocalization compared to the smaller  $\sigma$ -localization. Similarly, for the all-metal system,  $Al_4^{2-}$ , the ground state corresponds to a square

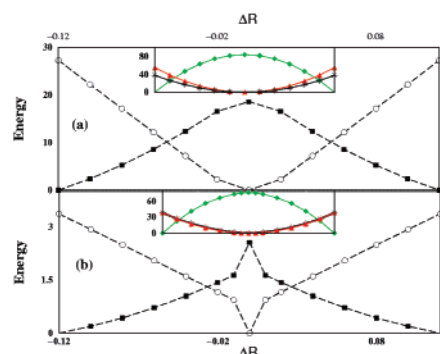


**Figure 2.** Same variation (including the inset) as in Figure 1 for (a)  $C_4H_4^{2+}$  and (b)  $Al_4^{2-}$ .

geometry with Al–Al bond length = 2.54 Å. This is readily understood from the plot as the  $\pi$ -destabilization associated with the distortion exceeds the stability in the  $\sigma$ -backbone due to distortion (Figure 2(b)) though again the energy scales for the  $\sigma$ - and  $\pi$ -distortion are comparable. Also, as a general rule, we find that the  $V_{ne}$  term favors distortion.

In summary, we have shown that all-metal molecular clusters such as  $Al_4Li_4$  and  $Ga_4Li_4$  are predominately  $\pi$ -antiaromatic although there is a significant contribution from the  $\sigma$ -aromaticity as well due to close proximity in  $\sigma/\pi$  energy scales compared to the equivalent organic systems. We believe that our analysis provides a tool for assignment of aromaticity/antiaromaticity in all-metal clusters.

**Acknowledgment.** S.K.P. thanks CSIR and DST, Government of India for research grant.

**Supporting Information Available:** Structures, Cartesian coordinates, ground-state energies, and complete ref 11. This material is available free of charge via the Internet at <http://pubs.acs.org>.

## References

- (1) Li, X.; Kuznetsov, A.; Zhang, H.-F.; Boldyrev, A. I.; Wang, L. *Science* **2001**, *291*, 859.
- (2) Li, X.; Zhang, H.-F.; Wang, L.-S.; Kuznetsov, A. E.; Cannon, N. A.; Boldyrev, A. I. *Angew. Chem. Int. Ed.* **2001**, *40*, 1867.
- (3) Kuznetsov, A.; Boldyrev, A. I.; Li, X.; Wang, L.-S. *J. Am. Chem. Soc.* **2001**, *123*, 8825.
- (4) Kuznetsov, A.; Birch, K.; Boldyrev, A. I.; Li, X.; Zhai, H.; Wang, L. *Science* **2003**, *300*, 622.
- (5) Datta, A.; Pati, S. K. *J. Am. Chem. Soc.* **2005**, *127*, 3496.
- (6) Chen, Z.; Corminboeuf, C.; Heine, T.; Bohmann, J.; Schleyer, P. V. R. *J. Am. Chem. Soc.* **2003**, *125*, 13930.
- (7) Ritter, S. *Chem. Eng. News* **2003**, *81*, 23.
- (8) Santos, J. C.; Andres, J.; Aizman, A.; Fuentealba, P. *J. Chem. Theory Comput.* **2005**, *1*, 83.
- (9) Shaik, S. S.; Hiberty, P. C. *J. Am. Chem. Soc.* **1985**, *107*, 3089.
- (10) Shaik, S. S.; Hiberty, P. C.; Lefour, J.-M.; Ohanessian, G. *J. Am. Chem. Soc.* **1987**, *109*, 363.
- (11) Frisch, M. J.; et al. Gaussian 03.
- (12) Boldyrev, A. I.; Wang, L.-S. *J. Phys. Chem. A* **2001**, *105*, 10759.
- (13) Hiberty, P. C.; Shaik, S. S.; Lefour, J.-M.; Ohanessian, G. *J. Org. Chem.* **1985**, *50*, 4657.
- (14) Jug, K.; Hiberty, P. C.; Shaik, S. *Chem. Rev.* **2001**, *101*, 1477.
- (15) Shaik, S.; Shurki, A.; Danovich, D.; Hiberty, P. C. *Chem. Rev.* **2001**, *101*, 1501.
- (16) Jug, K.; Koster, A. M. *J. Am. Chem. Soc.* **1990**, *112*, 6772.

CT0501351